Metrol. Meas. Syst., Vol. 29 (2022) No. 2, pp. 391–404
DOI: 10.24425/mms.2022.140032

PAN POLSKA AKADEMIA NAUK

METROLOGY AND MEASUREMENT SYSTEMS
Index 330930, ISSN 0860-8229
www.metrology.wat.edu.pl

M&MS

NEW METHOD TO ANALYZE RESOLUTION ACQUISITION FOR INTRAORAL SCANNERS

Alban Desoutter[1)], Gérard Subsol[2)], Eric Fargier[3)], Alexandre Sorgius[3)], Hervé Tassery[1)], Michel Fages[1)], Frédéric Cuisinier[1)]

1) *Univ. Montpellier, 163 rue Auguste Broussonnet, 34090 Montpellier, France* (✉ *alban34@yahoo.com*, +33 674 635 215, *herve.tassery@gmail.com*, *michel.fages@umontpellier.fr*, *frederic.cuisinier@umontpellier.fr*)
2) *Laboratory of Computer Science, Robotics and Microelectronics of Montpellier, 161 Rue Ada, 34095 Montpellier, France* (*gerard.subsol@lirmm.fr*)
3) *Laboratoire National de Métrologie et d'Essais, 1 Rue Gaston Boissier, 75724 Paris Cedex 15, France* (*eric.fargier@lne.fr*, *alexandre.sorgius@lne.fr*)

Abstract

In dentistry, 3D intraoral scanners (IOSs) are gaining increasing popularity in the production of dental prostheses. However, the quality of an IOS in terms of resolution remains the determining factor of choice for the practitioner; a high resolution is a quality parameter that can reduce error in the production chain. To the best of our knowledge, the evaluation of IOS resolution is not clearly established in the literature. This study provides a simple assessment of resolution of an IOS by measuring a reference sample and highlights various factors that may influence the resolution. A ceramic tip was prepared to create a very thin object with an edge smaller than the current resolution stated by the company. The sample was scanned with microCT (micro-computed tomography) and an IOS. The resulting meshes were compared. In the mesh obtained with the IOS, the distance between two planes on the edge was approximately 100 micrometers, and that obtained with microtomography was 25 micrometers. The curvature values were 27.46 (standard deviation – SD) 14.71) μm^{-1} and 5.18 (SD 1.16) μm^{-1} for microCT and IOS, respectively. These results show a clear loss of information for objects that are smaller than 100 µm. As there is no normalized procedure to evaluate resolution of IOSs, the method that we have developed can provide a positive parameter for control of IOSs performance by practitioners.

Keywords: resolution, intra oral scanner, mesh, MicroCT.

1. Introduction

3D intraoral scanners (IOSs) appeared in dentistry in the 1970s and were used to scan the tooth surface and to produce dental crowns [1] with a milling machine. The IOS is a medical device composed of a handheld 3D scanner (hardware) connected to a computer and software. The goal is to make precise three-dimensional measurements of an object in the mouth. The information

Article history: received December 16, 2021; revised February 24, 2022; accepted March 3, 2022; available online April 21, 2022.

collected is processed by software that reconstructs the three-dimensional (3D) model of the desired structures [2]. The most widely used digital open format for mesh is the *Standard Tessellation Language* (STL). Gradually, IOSs entered dental clinical practice either connected to a digital milling machining [3] or connected via the Internet to prosthetic laboratories.

Presently, IOSs are used to obtain study models of prostheses [4] and to generate impressions necessary for modeling and fabrication of a whole series of restorations, such as single crowns [5], fixed partial dentures [6], and in selected cases, complete fixed arches [7]. IOSs are also used in maxillofacial surgery, where the IOS is integrated in guided surgery procedures [8], and in orthodontics for fabrication of aligners and different customized orthodontic devices [9].

Originally, old models of IOSs required a powdering of TiO2 to suppress the light. Although this is no longer necessary today [10], powder coating may prove useful in the case of an optical impression of highly reflective surfaces such as metal prostheses.

An accurate 3D representation of teeth anatomy is the main objective of all IOSs [11]. Some questions related to creating a 3D mesh corresponding to teeth or a full arch are as follows:

1. What is the difference between reality and the 3D data acquired by the system and reconstructed by the algorithm?
2. What is the reproducibility level of the IOS?
3. What is the minimal detail size than can be recorded by an IOS?
4. Does this minimum size allow the acquisition of small structures of small dental reliefs such as perikymata?
5. Is it the minimum acceptable to produce a clinically acceptable dental crown?

For the two first questions corresponding to trueness and accuracy, several studies have been performed and published that provide some indication of the performances of IOSs [12–18], [19, p. 12], [20–24]. However, the third group of questions has not been addressed.

Accuracy was defined in 1997 by the *Joint Committee for Guides in Metrology* (JCGM) as the "closeness of agreement between a measured quantity value and a true quantity value of a measurand". Trueness was defined as: "closeness of agreement between the average of an infinite number of replicate measured quantity values and a reference quantity value", and resolution was defined as the "smallest change in a quantity being measured that causes a perceptible change in the corresponding indication". For a device that reconstructs volume, its resolution is the smallest object detected by the camera, or the smallest detail recordable.

To evaluate the accuracy and trueness, studies compared 3D models reconstructed from IOSs and 3D reference models (obtained with a measuring machine, a high-resolution scanner or microtomography). Variations among several acquisitions with an IOS provide information on the accuracy of the system, and the deviation between the IOS and reference acquisitions provides the trueness. In 2012, a study was conducted on the accuracy of three intraoral scanners (Cerec, iTero and Lava COS) [12]. The distances obtained with IOSs were compared to those obtained with an optical 3D measuring machine. Another comparison study between crown gap computer-aided manufactured with three different techniques: intra oral scanner, extraoral scanner and extraoral point laser scanner, showed statistical differences. As a result an advantage of the extraoral scanner over the other devices was proved [13].

In a 2014 study, a full arch with 14 abutments was digitalized with four commercial IOSs (iTero, CEREC AC Bluecam, Lava C.O.S., and Zfx IntraScan) and compared to 3D meshes obtained from an industrial scanner [14]. In the same year, no statistical difference was found when comparing two scanners performance (intra and extra oral) in terms of accuracy and precision) [15]. Another paper reported the study of an epoxy model and reference was provided by *micro-computed tomography* (microCT) [16]. A whole *Computer Aided Design – Computer Aided Manufacturing* (CAD-CAM) system, from intraoral scanning to 3D printing of the prosthesis

with the production unit, was also evaluated [17, 18]. An ISO standard has also been published to standardize methods for determining the accuracy of CAD-CAM systems. However, these tests require "a digitizing device in which the object is mounted relative to the optical or mechanical-contact system and, therefore, do not apply to hand-held scanning devices" [19].

In 2017, a perfectly flat wafer was used to determine IOS noise, which is the sum of the practitioner and optical errors, electronic and software noise [20]. The *measured roughness* (RMS) of a perfectly flat surface remains a valuable indicator for determining the noise of an IOS. A recent systematic review collected 32 studies on IOSs and concluded that accuracy is better with a low span of scanning on a surface with minimal irregularities [21]. A 2017 review of the literature notes that resolution of acquisition "is also important" and "depends on the cameras inside the scanner" but it does not note that there are no laboratory studies that approximate its [22].

Concerning the objects manufactured with CAD-CAM, a systematic review from 2020 concludes that removable partial denture framework fabrication has better accuracy when compared to traditional impressions, with gap clinically acceptable [23]. Another review highlights interest in microCT imaging in CAD-CAM dentistry, in particular as high resolution tool to evaluate the marginal gap or shape and volume to improve the quality of prostheses [24], which indicates that there is no clear scientific study on the resolution of IOSs and that the only data available is that given by the manufacturers.

While many studies have been published to evaluate the accuracy of IOSs, it is a combination of trueness and precision as they are defined below:

Accuracy: closeness of agreement between a quantity value obtained by measurement and the true value of the measurand;

Trueness: the closeness of agreement between the average value obtained from a large series of test results and an accepted reference value;

Precision: the closeness of agreement between independent test results obtained under stipulated conditions results and an accepted reference value [25];

Precision was studied by repeated measurements of the same sample and by evaluation of the distribution of such values. Trueness was studied by comparing the mesh obtained with an IOS and reference acquisition systems (such as a table scanner, microCT, *etc.*). No method to approximate the previously defined notion of resolution, for these cameras, is actually present in the literature.

Therefore, the aim of this study is to propose a reference object and a method to perform a set of calculations evaluating the IOS resolution.

So, a ceramic tip scanned by a reference system (microCT) was used. Then, this reference form was scanned with an IOS to evaluate the cropping by the IOS on the ridge line. This approach allowed the determination of the smallest element that the IOS can detect. The distance and curvature, which is an approximation of the second order of the surface and can be defined locally, were obtained.

2. Materials and methods

2.1. Materials

2.1.1. Ceramic tip preparation

Vita Mark II feldspathic ceramic blocks (Vita Zahnfabrik) for CAD-CAM systems were longitudinally sectioned using a high-speed diamond saw (Isomet 2000) to obtain 4 cm match-like specimens. Then, the specimen was cut 1 cm from the top and the ceramic was beveled. The cut face was polished with abrasive discs with up to 1200 grit followed by polishing with

diamond pastes of 0.25 and 0.1 µm particle sizes using a polishing machine (Escil). Thereafter, the samples were cleaned ultrasonically in a distilled water bath.

2.1.2. Intraoral scanner

The CS3600 IOS from Carestream (Rochester) is a powder-free system. It is a confocal parallel system with a green laser light and a pinhole to select a focal plane. The light projected on the tooth is collected on a CMOS (*Complementary Metal-Oxide-Semiconductor*) consisting of a 1.3 cm sensor that transforms light into an electric signal. A motor quickly moves the focal plane and a high intensity signal is collected to reconstruct the 3D mesh. During 3D recording, the intraoral scanner can capture HD photographs with 4 LEDs (blue, green, red, and UV) for realistic tooth reconstruction. The IOS is operated by a CAD-CAM experienced clinician (Fig. 1).

2.1.3. MicroCT

X-ray tomography of the tip was performed with an EasyTom 150 kV system (RX Solution). The X ray source had a voltage of 70 kV and a voxel size of 5.4 micrometers and an aluminum filter was placed front of the X ray generator. Regular calibration procedure assured an alignment of the machine and an error of the measurement of less than 0.5 micrometer.

2.1.4. Optical measuring machine

The Excel 502 Multisensor Measuring machine (Windsor) provides high-speed and accurate measurements. This instrument allows the measurement of $400 \times 500 \times 250$ mm specimens with an x, y accuracy of $(2.8 + L/200)$ µm and a z accuracy of $(3.0 + L/100)$ µm, where L is the specimen length measured in mm, and a scale resolution of 0.1 µm. This machine was only used to evaluate the curvature of the tip on the edge; a 2D image was captured to approximate an order of magnitude of the sample.

2.2. Methods

2.2.1. Mesh extraction

The IOS 3D mesh was directly imported from a computer connected to the scanner via the operating software CS Restore (Version number 6.14.7.3, Carestream, Rochester). The 16-bit tiff microtomography slice files (1,315 files) were processed with Fiji software (v1.51, the National Institutes of Health) and the threshold was determined using the gray shade mean value of the internal material of the tip. The images were then converted into the 8-bit format. The resulting image files were visualized with a plug-in 3DViewer in Fiji software [26] that allows the computation of a 3D mesh corresponding to the surface of the scanned object in an STL binary file. To determine the threshold between the air and the object, a mean value of the gray shade of object was extracted from a 2D tiff image with the Fiji software.

2.2.2. Data analysis: mesh comparisons

The alignment of the meshes (IOS mesh and microCT mesh) and the calculation of the distance were performed with CloudCompare software (version 2.10-alpha, EDF R&D). First, the best fit record was automatically calculated with an algorithm by minimizing the distance between each mesh vertex. Then, each vertex of the 3D mesh was projected onto the nearest face (triangle) of the reference mesh. The distance to the vertex was measured and a color look-up-table was used to visualize the distances. Such a method allowed us to visualize the distances between the IOS and the microCT meshes.

Metrol. Meas. Syst., Vol. 29 (2022), No. 2, pp. 391–404
DOI: 10.24425/mms.2022.140032

2.2.3. Method for resolution approximation

Resolution is the average the minimum distance between the two faces of the tip or the minimal curvature of the tip determined by the IOS device. To achieve this measurement, we have developed a set of two calculations.

• Distance between two tip faces

No simple method exists to automatically select the vertex immediately before the curvature on the edges of the tip. The distances were calculated with the Meshlab software tool by the selection of the vertex of interest. To minimize error by the manipulator, 30 measurements were collected for each 3D image and means and standard deviations were calculated.

• Curvature calculation

The curvature of the tip top was calculated with a specific function in the Meshlab software using the discrete mean curvature of a normal operator given by the following formula shown in [27]:

$$K(x_i) = \frac{1}{2A_{\text{Mixed}}} \sum_{j \in N_1(i)} \left(\cot \alpha_{ij} + \cot \beta_{ij}\right)(x_i - x_j), \tag{1}$$

where A_{Mixed} is a normalization term that represents the area defined for each vertex of a non-obtuse triangle connected to the circumcenter point and for each vertex of an obtuse triangle connected to the midpoint of the edge opposite to the obtuse angle; a simple algorithm (pseudocode) allows full surface tiling; x_i is the position of the vertex where the curvature is evaluated, x_i is the difference in the first neighbors of vertex $N_1(i)$ and α_{ij} and β_{ij} are the angles opposite to the segment formed by the vertices i and j (Fig. 1d). The curvature was calculated for the vertex of interest on the edge of the top of our object. The selection is represented as a red area, as shown in Fig. 1a–1b.

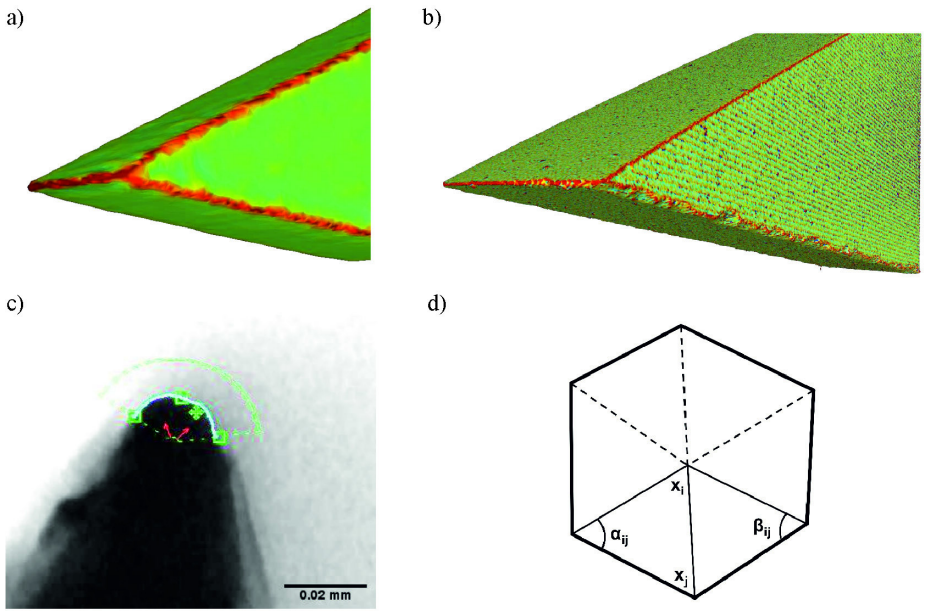

Fig. 1. a, b) Mesh obtained using the IOS and microCT, respectively; the red area corresponds to the highest curvature of the mesh, the green area corresponds to the flat part. c) Ceramic tip profile imaged with an optical measuring machine. d) Layout of a vertex and neighbors to explain the curvature calculation formula.

To avoid extreme values, calculations of the means were performed with a truncated value by discarding the 5th and 95th percentiles. Those values were compared with the value obtained with the optical confocal machine (Fig. 1c).

2.2.4. Statistical analysis

To compare the distance and curvature results, we performed one-way ANOVA using Sigmaplot version 11.0 (Systat Software Inc, San Jose, USA).

3. Results

3.1. Distance between two tip faces

The mean, median and *standard deviation* (SD) of the distances between the upper and lower planes of the tip which represent the smallest volume visible by the IOS or microCT are presented in the top panel of Fig. 2. The microCT mean measurement result was 25.98 micrometers, and the values determined by the camera ranged between 89.67 and 124.28 micrometers (Table 1).

Table 1. Mean, standard deviation (SD) and median distances between the two tip planes; superscript letters indicate a statistically significant difference. Description of upper indexes a, b, c. . .

	a. Micro CT	**b. IOS test 1**	**c. IOS test 2**	**d. IOS test 3**	**e. IOS test 4**	**f. IOS test 5**
Mean (µm)	$25.98^{b,c,d,e,f}$	$121.22^{a,d,f}$	110.61^{a}	$89.67^{a,b,e}$	$124.28^{a,d}$	$91.67^{a,b}$
SD (µm)	7.10	20.85	22.70	14.19	31.18	25.03
Median (µm)	24.50	118.50	109.50	89.50	124.50	86.00

Figure 2 represents the results in the form of a boxplot, emphasizing the different distributions and reproducibility of measurements of the same object with the IOS.

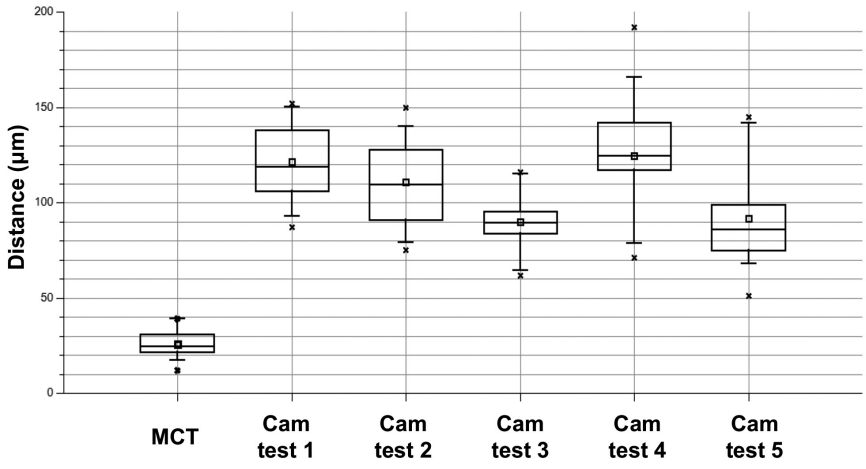

Fig. 2. Distances between two planes of the meshes of the tip recorded by microCT and the CS3600 camera (IOS) for 5 different acquisitions (tests 1–5) Rectangle: 25% to 75%. Whiskers: 5–95% range. Square: mean value. Point: min and max value.

Metrol. Meas. Syst., Vol. 29 (2022), No. 2, pp. 391–404
DOI: 10.24425/mms.2022.140032

3.2. Curvature

The curvature and the distribution of the mesh on the tip in the ROI (region of interest) are presented in Fig. 3. The 20% truncated mean of curvature for microCT was 27.46 (SD 14.71) μm^{-1}, and the range was between 3.57 and 7.05 μm^{-1} for the camera (Table 2).

Table 2. Mean, standard deviation (SD) and median curvature; superscript letters indicate statistically significant differences. Description of upper indexes a, b, c. . .

	a. Micro CT	**b. IOS test 1**	**c. IOS test 2**	**d. IOS test 3**	**e. IOS test 4**	**f. IOS test 5**
Truncated mean (μm^{-1})	$27.46^{b,c,d,e,f}$	$4.79^{a,c}$	$7.05^{a,e,f,b}$	$6.23^{a,e}$	$3.57^{a,c,d}$	$4.29^{a,c}$
SD (μm^{-1})	14.71	2.79	3.56	3.96	1.54	2.13
Median (μm^{-1})	27.02	4.68	7.06	6.28	3.44	4.17

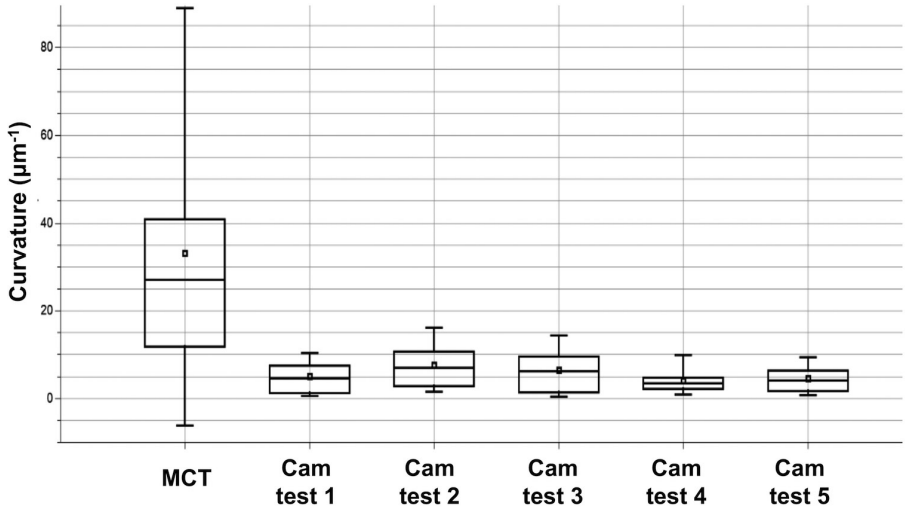

Fig. 3. Curvature of the meshes of the tip recorded by microCT and the CS3600 camera (IOS) for 5 different acquisitions (tests 1–5) Rectangle: 25% to 75%. Whiskers: 5–95% range. Square: mean value. Point: min and max value.

3.3. Mesh registrations

Meshes extracted from microCT and IOS have been successfully registered and algorithm create a convergence with 3 iterations of the soft (Meshlab) algorithm. Figure 4 shows an example of such registration. Figure 4c represents a color map of the projected distance, connected with look up table. Figure 5 represents quantitative results with a box plot for the 5 tests realized on the same sample.

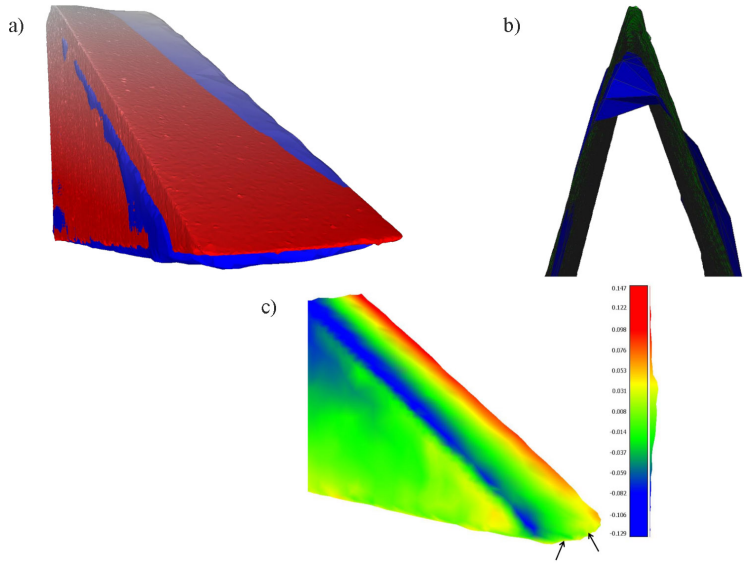

Fig. 4. a) registration/superposition of the mesh recorded from the microCT image and the CS3600 camera; b) detail of the superposition on a region of interest; c) colored map representation of distance calculated by projection of the camera mesh vertex on microCT mesh faces. Black arrows: the distance values of interest.

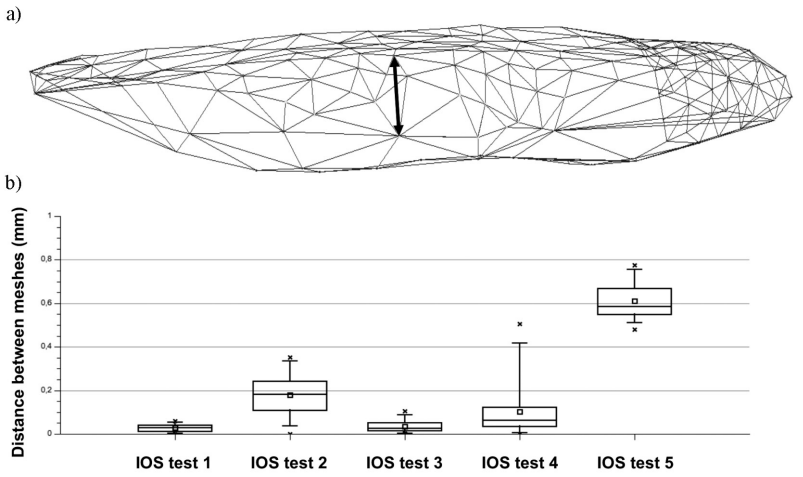

Fig. 5. a) scheme of distance calculation between two faces with IOS mesh; b) Distance between mesh for the microCT and the CS3600 camera (IOS) for 5 different acquisitions (test 1–5) Box plot: rectangle: 25% to 75%. Whiskers: 5–95% range. Square: mean value. Cross: min and max values. X axis: parameter acquisition (angulation and direction 1 or 2) and calculated area (W = whole mesh; CR = central region of mesh). MicroCT and the CS3600 (IOS) camera were used for 5 different acquisitions (tests 1-5).

3.4. Top View Comparison

Figure 6 presents images of qualitative comparison of loss information, by superposition of edge extracted of optical measuring tip machine (a) and microCT (b) and IOS (c) top view of the tip.

Metrol. Meas. Syst., Vol. 29 (2022), No. 2, pp. 391–404
DOI: 10.24425/mms.2022.140032

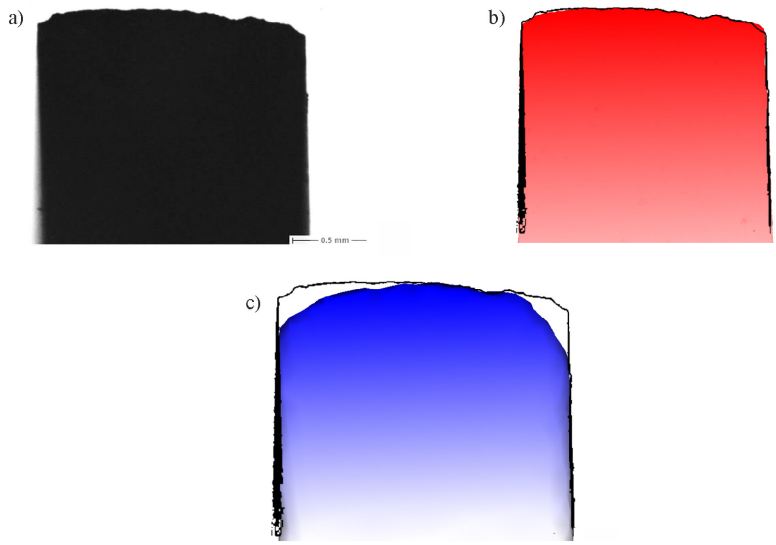

Fig. 6. Top view of the tip visualized with a) an optical measuring machine, b) microCT and c) the CS3600 camera. Black line in b) and c) the edge of the image obtained with the optical machine in a). The blank in b) and c), corresponds to the difference between the optical measuring machine edge and the 3D image scanned with microCT and the IOS and represents loss of information.

4. Discussion

4.1. Resolution

IOSs and microCT are systems used to discretize representation of objects. In our model, the distance that separates the points at the end of each plane of the tip represents the resolution of the system studied. Indeed, the capacity of an IOS to reproduce the detail of a tip is equivalent to the minimal size that can be recorded. As shown in Fig. 2, this distance is 25.98 micrometers (SD 7.1) for microCT, ranges from 89.67 (SD 14.19) to 124.28 (SD 31.18) micrometers for the IOS studied, and is 8.6 micrometers as measured with an optical measuring machine. We note the dispersion of the results for IOS acquisitions. This dispersion illustrates the difficulty in performing reliable acquisitions with an IOS. Manual handling of the camera influences the results and alters the reproducibility and quality of the meshes obtained. This fact is supported by the p-value of the statistical test, as shown in the Table 1 (superscript letters). These results differ very much from the resolution stated by the company. In the case of the CS3600 camera, no resolution was stated in the commercial documents or the website of the Carestream Company; only the term “high resolution” was used. Those results, which greatly diverged from those of the optical measuring machine, could be explained by the acquisition method, which merged many images to create a complete mesh of the object. Also, this method could smooth the angulations. The acquisition of an image at a high rate of speed, as recording a movie, encourages the use of such instrument by practitioners. First generation IOSs recorded individual images [28]. With a pixel size and resolution of 5.4 micrometers, micro tomography has a very high performance to acquire a sample mesh. This allows us to have a model close to reality to compare with the IOS, assuming that the resolution obtained with the camera will necessarily be much greater than the mesh obtained with microCT. The results obtained presently do not prevent gluing the patient

prothesis crowns, but this could cause some problem as they can lead to inaccuracies affecting future machining of prosthetic crowns, such as milling defects or over-milling.

The smoothing of edges with an IOS is clearly visible in Fig. 6 where tips are oriented in the same "top view" for the three techniques: optical machine (a), microCT (b) and IOS (c). Superposition of the image obtained with the optical measurement machine image, which is considered the closest condition to reality, and the two other techniques emphasize the edge smoothing produced by the IOS.

With these results, it is possible to study the roughness of teeth in vivo. Indeed, the perikymata are between 50 and 100 micrometers, and such structures are within the resolution established in this experimental setup. The present results can also explain a part of divergence between the true value and recorded value even if it is weak. Indeed, CS 3600 have been evaluated as better compared to other IOS in published paper accuracy of such medical device [29].

4.2. Curvature

The results of the measurements described above were confirmed with the curvature calculations detailed in Fig. 3. The distance values are linked to the curvature of the tip. The tip used in this experiment is not perfectly flat and smooth. The ceramic is very hard and it is clearly visible on the confocal optical image of the tip profile that the top is jagged because of the milling. The experimental difficulty in obtaining a perfect tip leads to extreme values in the mean curvature calculation. The values that correspond to negative curvatures are eliminated and only the values that represent the round part of the top of the tip are selected. The distance that separates the two planes is large and the curvature is small. As expected, the curvature on the tip in the microCT mesh is clearly greater than the curvature observed in IOS meshes (p-value less than 0,05 for the comparison of the 5 tests with the IOS). This kind of measure has a large spread as illustrated by the whisker position and the value of the SD reported. This finding can be explained by the non-homogeneity of the mesh in the ROI (region of interest); some points have first neighbors in a very flat localization or in a punctual negative curvature region. Therefore, the truncated mean is needed to avoid extreme positions.

4.3. Registration

The method of registration between two surfaces in 3D must be discussed here. Indeed, the results obtained represent the distance between the top of the tips in images obtained with microCT and IOS. However, these results were difficult to obtain. In theory, such a method could approximate the loss of material that is not recorded with the IOS as compared to the microCT reference mesh. First, to register the two surfaces, the ROI must be cropped to obtain two similar meshes and to avoid error in calculation. This step is not automatic or performed by a rigorous methodology. The resulting numbers and sizes of triangles for a similar region are very different; with the IOS, 1167 vertices and 2280 triangles are recorded; with microCT, 322,274 vertices and 673,401 triangles are recorded. The mean size of a triangle is 44 square micrometers with microCT and 12,340 square micrometers with the IOS. Therefore, cutting of the two meshes to obtain a similar geometry can influence the result. Second, we observed that the mesh representing the tip, scanned with the IOS is twisted compared to that inspected with the microCT. The problem of tip distortion by the IOS must be further studied.

The artifacts of IOSs have previously been highlighted in several studies that revealed many sources of distortions due to instability of the scanner or angulation problems.

5. Conclusions

This method is the first to calculate the IOS resolution. It allows development of a standard procedure to evaluate their performance. The results are obtained by calculating the distance between planes which are correlated with the curvature of the tip. It constitutes a good method for selecting commercial systems. The results demonstrate a clear difference between the actual object and the meshes obtained with the IOS and its associated software. The present study is limited by the evaluation of the loss of information by the IOS due to the difficulties in obtaining good meshes registration with a twisted IOS mesh. It is a first step to create a process including a physical device and software to control stability of the system over time and to compare IOS systems. A method is under study to automatically evaluate this performance with a finely parameterized object.

Acknowledgements

3D data acquisitions were performed using the µCT (microCT) facilities of the MRI platform member of the national infrastructure France-BioImaging supported by the French National Research Agency (ANR-10-INBS-04, "Investments for the Future"), and by the Labex CEMEB (grant ANR-10-LABX-0004) and the NUMEV (grant ANR-10-LABX-0020).

References

[1] Duret, F., & Termoz, C. (1987). *Method of and apparatus for making a prosthesis, especially a dental prosthesis* (U.S. Patent No. 4,663,720). https://patents.google.com/patent/US4663720A/en

[2] Ting-Shu, S., & Jian, S. (2015). Intraoral digital impression technique: a review. *Journal of Prosthodontics*, *24*(4), 313–321. https://doi.org/10.1111/jopr.12218

[3] Beuer, F., Schweiger, J., & Edelhoff, D. (2008). Digital dentistry: an overview of recent developments for CAD/CAM generated restorations. *British Dental Journal*, *204*(9), 505–511. https://doi.org/10.1038/sj.bdj.2008.350

[4] Zhang, F., Suh, K. J., & Lee, K. M. (2016). Validity of intraoral scans compared with plaster models: an in-vivo comparison of dental measurements and 3D surface analysis. *PloS One*, *11*(6), e0157713. https://doi.org/10.1371/journal.pone.0157713

[5] Tsirogiannis, P., Reissmann, D. R., & Heydecke, G. (2016). Evaluation of the marginal fit of single-unit, complete-coverage ceramic restorations fabricated after digital and conventional impressions: A systematic review and meta-analysis. *The Journal of Prosthetic Dentistry*, *116*(3), 328–335. https://doi.org/10.1016/j.prosdent.2016.01.028

[6] Almeida e Silva, J. S., Erdelt, K., Edelhoff, D., Araújo, É., Stimmelmayr, M., Vieira, L. C. C., & Güth, J. F. (2014). Marginal and internal fit of four-unit zirconia fixed dental prostheses based on digital and conventional impression techniques. *Clinical Oral Investigations*, *18*(2), 515–523. https://doi.org/10.1007/s00784-013-0987-2

[7] Ender, A., Attin, T., & Mehl, A. (2016). In vivo precision of conventional and digital methods of obtaining complete-arch dental impressions. *The Journal of Prosthetic Dentistry*, *115*(3), 313–320. https://doi.org/10.1016/j.prosdent.2015.09.011

[8] Lanis, A., & Del Canto, O. Á. (2015). The combination of digital surface scanners and cone beam computed tomography technology for guided implant surgery using 3Shape implant studio software: a case

history report. *International Journal of Prosthodontics*, *28*(2), 169–178. https://doi.org/10.11607/ijp.4148

[9] Vasudavan, S., Sullivan, S. R., & Sonis, A. L. (2010). Comparison of intraoral 3D scanning and conventional impressions for fabrication of orthodontic retainers. *Journal of Clinical Orthodontics*, *44*(8), 495–497. https://pubmed.ncbi.nlm.nih.gov/21105587/

[10] Li, H., Lyu, P., Wang, Y., & Sun, Y. (2017). Influence of object translucency on the scanning accuracy of a powder-free intraoral scanner: A laboratory study. *The Journal of Prosthetic Dentistry*, *117*(1), 93–101. https://doi.org/10.1016/j.prosdent.2016.04.008

[11] International Organization for Standardization (2006). *Dentistry – Intraoral camera* (ISO Standard No. 23450:2021). https://www.iso.org/standard/75616.html

[12] Van der Meer, W. J., Andriessen, F. S., Wismeijer, D., & Ren, Y. (2012). Application of intra-oral dental scanners in the digital workflow of implantology. *PloS ONE*, *7*(8), e43312. https://doi.org/10.1371/journal.pone.0043312

[13] Trifković, B., Budak, I., Todorović, A., Hodolić, J., Puškar, T., Jevremović, D., & Vukelić, Đ. (2012). Application of replica technique and SEM in accuracy measurement of ceramic crowns. *Measurement Science Review*, *12*(3), 90–97. https://doi.org/10.2478/v10048-012-0016-7

[14] Patzelt, S., Emmanouilidi, A., Stampf, S., Strub, J. R., & Att, W. (2014). Accuracy of full-arch scans using intraoral scanners. *Clinical Oral Investigations*, *18*(6), 1687–1694. https://doi.org/10.1007/s00784-013-1132-y

[15] Trifkovic, B., Budak, I., Todorovic, A., Vukelic, D., Lazic, V., & Puskar, T. (2014). Comparative analysis on measuring performances of dental intraoral and extraoral optical 3D digitization systems. *Measurement*, *47*, 45–53. https://doi.org/10.1016/j.measurement.2013.08.051

[16] Nedelcu, R., Olsson, P., Nyström, I., Rydén, J., & Thor, A. (2018). Accuracy and precision of 3 intraoral scanners and accuracy of conventional impressions: A novel in vivo analysis method. *Journal of Dentistry*, *69*, 110–118. https://doi.org/10.1016/j.jdent.2017.12.006

[17] Magnus Lilja, C. P. O., Sei, L. M., & Oberg, T. (1995). Volumetric determinations with CAD/CAM in prosthetics and orthotics: errors of measurement. *Journal of Rehabilitation Research and Development*, *32*(2), 141–148.

[18] Parsell, D. E., Anderson, B. C., Livingston, H. M., Rudd, J. I., & Tankersley, J. D. (2000). Effect of camera angulation on adaptation of CAD/CAM restorations. *Journal of Esthetic and Restorative Dentistry*, *12*(2), 78–84. https://doi.org/10.1111/j.1708-8240.2000.tb00204.x

[19] International Organization for Standardization. (2015). *Dentistry — Digitizing devices for CAD/CAM systems for indirect dental restorations – Test methods for assessing accuracy* (ISO Standard No. 12836:2015). https://www.iso.org/standard/68414.html

[20] Desoutter, A., Yusuf Solieman, O., Subsol, G., Tassery, H., Cuisinier, F., & Fages, M. (2017). Method to evaluate the noise of 3D intra-oral scanner. *PloS ONE*, *12*(8), e0182206. https://doi.org/10.1371/journal.pone.0182206

[21] Abduo, J., & Elseyoufi, M. (2018). Accuracy of Intraoral Scanners: A Systematic Review of Influencing Factors. *The European Journal of Prosthodontics and Restorative Dentistry*, *26*(3), 101–121. https://doi.org/10.1922/ejprd_01752abduo21

[22] Mangano, F., Gandolfi, A., Luongo, G., & Logozzo, S. (2017). Intraoral scanners in dentistry: a review of the current literature. *BMC Oral Health*, *17*, 149. https://doi.org/10.1186/s12903-017-0442-x

[23] Pereira, A. L. C., de Medeiros, A. K. B., de Sousa Santos, K., de Almeida, É. O., Barbosa, G. A. S., & Carreiro, A. D. F. P. (2021). Accuracy of CAD-CAM systems for removable partial denture framework fabrication: A systematic review. *The Journal of Prosthetic Dentistry*, *125*(2), 241–248. https://doi.org/10.1016/j.prosdent.2020.01.003

[24] Gulati, V. (2020). Implementation of Micro CT in CAD/CAM dentistry for image processing and soft computing: a review. *In Journal of Physics: Conference Series* (Vol. 1432, No. 1, p. 012079). IOP Publishing. https://doi.org/10.1088/1742-6596/1432/1/012079

[25] Menditto, A., Patriarca, M., & Magnusson, B. (2007). Understanding the meaning of accuracy, trueness and precision. *Accreditation and Quality Assurance*, *12*(1), 45–47. https://doi.org/10.1007/s00769-006-0191-z

[26] Schmid, B., Schindelin, J., Cardona, A., Longair, M., & Heisenberg, M. (2010). A high-level 3D visualization API for Java and ImageJ. *BMC Bioinformatics*, *11*(1), 1–7. https://doi.org/10.1186/1471-2105-11-274

[27] Meyer, M., Desbrun, M., Schröder, P., & Barr, A. H. (2003). Discrete differential-geometry operators for triangulated 2-manifolds. In H.-C. Hege, & K. Polthier (Eds.), *Visualization and mathematics III* (pp. 35–57). Springer. https://doi.org/10.1007/978-3-662-05105-4_2

[28] Cooka, K. T., & Fasbinderb, D. J. (2012). Accuracy of CAD/CAM Crown Fit with Infrared and LED Cameras. *International Journal of Computerized Dentistry*, *15*, 315–326. (in German)

[29] Imburgia, M., Logozzo, S., Hauschild, U., Veronesi, G., Mangano, C., & Mangano, F. G. (2017). Accuracy of four intraoral scanners in oral implantology: a comparative in vitro study. *BMC Oral Health*, *17*(1), 1–13. https://doi.org/10.1186/s12903-017-0383-4

Alban Desoutter obtained his first M.Sc. in Physics for Biomedical Science in 2015 and then a second one in Theoretical Physics/Nanosciences in 2017, both from the University of Montpellier, France. He is currently working in the Bioengineering and Nanoscience Laboratory at the University of Montpellier as a technical assistant. He is in charge of the confocal Raman and Brillouin microscopy. He is currently working on a thesis on Brillouin scattering optical setups. He also works on intraoral optical cameras and microtomography.

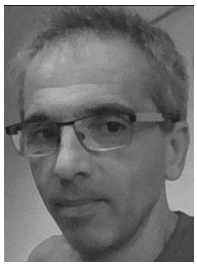

Gérard Subsol obtained an Engineer Diploma and a Ph.D. in Computer Science from the Ecole Centrale de Paris in 1991 and in 1995, respectively. Since November 2006, he has been a CNRS Research Associate with the ICAR research team at the Laboratory of Computer Science, Robotics, and Microelectronics (LIRMM) in Montpellier, France. He is currently working on several applications of 2D and 3D visual data processing and modelling.

Eric Fargier received his engineer diploma from the National School of Engineers in Tarbes (ENIT) in 1984. Presently, he is Head of the Dimensional Metrology Department of the National Laboratory of Metrology and Testing (LNE) with two local centers in Nimes and Paris providing research and calibration services for the industrial companies. He is also a CMM (coordinate measuring machine) accreditation expert at the French Accreditation Committee (COFRAC).

Hervé Tassery received his Ph.D. in biomaterials from Aix Marseille University in 2001. Currently, he is a professor at the Restorative and Preventive Department of Marseille Dental School of Aix-Marseille University. His major fields of interest are in cariology, fluorescence devices, minimally invasive dentistry, and clinical research. He works at the Laboratory of Bio-nanotechnology of Montpellier 1 University, as Head of the Biophotonic and Dental Diagnosis Team. His recent research interest has focused on improving links between fundamental researches, clinical researches and clinical applications.

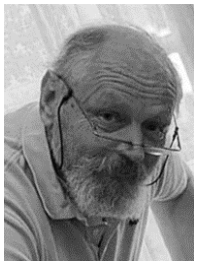

Frédéric Cuisinier first graduated as a dentist and entered the National Board of Periodontology. After receiving a Master of Science, in 1990 he obtained a Ph.D. in High Resolution Electron Microscopy of bone and enamel crystal formation with Prof. Robert Frank as his supervisor. He has been full time professor at Montpelier University since 2005. He has created the LBN (Laboratory of Bioengineering and Nanoscience) at Montpellier University and is its acting director.

Michel Fages received his Ph.D. degree from the University of Szeged (Hungary) in 2013. He is currently Full Professor and Head of the Prosthodontic Department in the Faculty of Odontology of Montpellier, France, and Head of the Cad/Cam-Prosthetic Medical Department in the Dental Care Center of the University Hospital of Montpellier. His research activity focuses on the biomechanics of the tooth reconstructed with CAD/CAM and dental CAD /CAM technologies.

Alexandre Sorgius obtained the M.Sc. degree in mechanical engineering from the Supméca Institute of Mechanics, Paris, in 2013. He is currently Project Engineer in dimensional metrology at the National Laboratory of Metrology and Testing (LNE). His activity focuses on developing and applying methods for calibration of measuring instruments and measurement of 3D parts.